MOLECULAR AND CELLULAR BIOLOGY, Jan. 2005, p. 88–99 Vol. 25, No. 1
0270-7306/05/$08.00+0 doi:10.1128/MCB.25.1.88–99.2005

Disruption of the *langerin/CD207* Gene Abolishes Birbeck Granules without a Marked Loss of Langerhans Cell Function

Adrien Kissenpfennig,[1] Smina Aït-Yahia,[2] Valérie Clair-Moninot,[2] Hella Stössel,[3] Edgar Badell,[4] Yann Bordat,[4] Joanne L. Pooley,[5] Thierry Lang,[6] Eric Prina,[6] Isabelle Coste,[2] Olivia Gresser,[1] Toufic Renno,[2] Nathalie Winter,[4] Geneviève Milon,[6] Ken Shortman,[5] Nikolaus Romani,[3] Serge Lebecque,[2] Bernard Malissen,[1]* Sem Saeland,[2]* and Patrice Douillard[2]

Centre d'Immunologie de Marseille-Luminy, INSERM-CNRS-Université de la Méditerranée, Parc Scientifique de Luminy, Marseille,[1] Laboratory for Immunological Research, Schering Plough, Dardilly,[2] and Unité d'Immunophysiologie et Parasitisme Intracellulaire[6] and Unité de Génétique Mycobactérienne,[4] Institut Pasteur, Paris, France; Department of Dermatology, Innsbruck Medical University, Innsbruck, Austria[3]; and The Walter and Eliza Hall Institute of Medical Research, Victoria, Australia[5]

Received 2 August 2004/Returned for modification 3 September 2004/Accepted 10 October 2004

Langerin is a C-type lectin expressed by a subset of dendritic leukocytes, the Langerhans cells (LC). Langerin is a cell surface receptor that induces the formation of an LC-specific organelle, the Birbeck granule (BG). We generated a *langerin*$^{-/-}$ mouse on a C57BL/6 background which did not display any macroscopic aberrant development. In the absence of langerin, LC were detected in normal numbers in the epidermis but the cells lacked BG. LC of *langerin*$^{-/-}$ mice did not present other phenotypic alterations compared to wild-type littermates. Functionally, the *langerin*$^{-/-}$ LC were able to capture antigen, to migrate towards skin draining lymph nodes, and to undergo phenotypic maturation. In addition, *langerin*$^{-/-}$ mice were not impaired in their capacity to process native OVA protein for *I-A*^{b}-restricted presentation to CD4^{+} T lymphocytes or for *H-2K*^{b}-restricted cross-presentation to CD8^{+} T lymphocytes. *langerin*$^{-/-}$ mice inoculated with mannosylated or skin-tropic microorganisms did not display an altered pathogen susceptibility. Finally, chemical mutagenesis resulted in a similar rate of skin tumor development in *langerin*$^{-/-}$ and wild-type mice. Overall, our data indicate that langerin and BG are dispensable for a number of LC functions. The *langerin*$^{-/-}$ C57BL/6 mouse should be a valuable model for further functional exploration of langerin and the role of BG.

Dendritic cells (DC) are the most potent leukocytes to mediate the rapid initiation of a primary immune response (7). DC are bone marrow-derived leukocytes, localized in most tissues including primary and secondary lymphoid organs. In the periphery, most DC are in an immature state and are able to capture antigenic molecules via unique endocytic receptors or by fluid-phase macropinocytosis. This process generally leads to a first step of DC maturation, concomitant with their migration to secondary lymphoid organs. DC can subsequently activate naive CD4^{+} T or CD8^{+} T lymphocytes if peptides processed from native antigenic molecules are displayed on cell surface major histocompatibility complex (MHC) class II or I molecules in conjunction with cosignaling molecules (40).

DC heterogeneity is a common feature of mice and humans. Precursor cell populations, anatomical localization, morphology, phenotype, and functions determine the type of DC. However, the origin of different DC subsets is still controversial (4). A particular subset of DC is represented by Langerhans cells (LC), which are immature DC present in the epidermis and mucosal epithelium (53, 71). LC can be generated either from myeloid precursors (77, 78) or from CD4^{low} lymphoid precursors (2). LC express a number of cell surface receptors including CD205/DEC205, Fcγ and Fcε receptors, and langerin/CD207 (70, 72).

Langerin is a C-type lectin oriented in a type II configuration and featuring a single carbohydrate recognition domain in its extracellular region (72). Langerin molecules oligomerize as trimers at the cell surface and display Ca^{2+}-dependent binding specificity for mannose, *N*-acetyl-glucosamine, and fucose (61, 72). Langerin is a potent inducer of Birbeck granules (BG), the hallmark organelles of LC, which consist of pentalamellar and zippered membranes at the electron microscopic level (12, 75). In addition to inducing BG formation, langerin is an endocytic receptor involved in the trafficking of exogenous mannosylated ligands from the cell surface into intracellular BG compartments (71).

To further explore the role of langerin and BG, we generated C57BL/6 mice with a targeted disruption of the *langerin* gene. Although MHC class II-positive LC were detected in normal numbers in the epidermis of these mice, they did not have detectable cytoplasmic BG. Yet LC functions, such as migration, endocytosis (capture of macromolecules), antigen processing, and presentation to MHC class I- and class II-restricted T lymphocytes, were not altered. Finally, *langerin*$^{-/-}$ and C57BL/6 wild-type control mice responded similarly to infections by microorganisms such as *Mycobacterium tubercu-*

* Corresponding author. Mailing address for Sem Saeland: Schering Plough, Laboratory for Immunological Research, 27, Chemin des Peupliers, BP 11, 69571 Dardilly cedex, France. Phone: 33 4 72 17 27 00. Fax: 33 4 78 35 47 50. E-mail: semsaeland@yahoo.fr. Mailing address for Bernard Malissen: Centre d'Immunologie de Marseille-Luminy, INSERM-CNRS-Université de la Méditerranée, Parc Scientifique de Luminy, 13288 Marseille Cedex 9, France. Phone: 33 491 26 94 78. Fax: 33 491 26 94 30. E-mail: bernardm@ciml.univ-mrs.fr.

losis and *Leishmania major* or to chemically induced skin carcinogenesis. Together, our data demonstrate that langerin and BG are dispensable for a number of LC functions.

MATERIALS AND METHODS

Mice. C57BL/6J mice were purchased from Charles River Breeding Laboratories (Saint Germain sur l'Arbresle, France) and used as wild-type controls. OT-I mice express a transgenic Vα2Vβ5 T-cell receptor (TCR) specific for the $OVA_{257–264}$ epitope in the context of *H-2K*^{b} (29). OT-II mice express a transgenic Vα2Vβ5 TCR specific for the $OVA_{323–339}$ epitope in the context of *I-A*^{b} (8) (both were kind gifts from Francis R. Carbone, University of Melbourne, Melbourne, Australia), and *langerin*$^{-/-}$ mice were bred and housed in the Charles River facility under specific-pathogen-free conditions. All experiments involving mice were conducted in accordance with protocols approved by French laws and European or Australian directives. Mice were used at 8 to 12 weeks of age.

***langerin*-null targeting vector construction.** The langerin targeting vector was constructed from a cosmid genomic clone isolated from a 129/Ola cosmid library as previously described (70). Briefly, a 2.9-kb KpnI-XhoI fragment (5′ homology arm containing 5′ flanking sequence and 80 bp of exon 1) and a 2.7-kb XhoI-BglII fragment (3′ homology arm containing 128 bp of exons 4 and 5 and 155 bp of exon 6) were simultaneously cloned into KpnI and BamHI sites of pBluescript II KS+ (Stratagene, La Jolla, Calif.). To assure complete elimination of langerin expression, the unique XhoI site was blunted by using a Klenow with exonuclease activity, and a *pgk*-neomycin cassette flanked by *loxP* sites was inserted blunt into the targeting vector. Sequence analysis of the neomycin insertion site revealed complete deletion of exon 1 (70 bp upstream of the ATG start codon) and partial deletion of exon 4. Finally, the targeting vector was abutted to a thymidine kinase expression cassette and linearized by a unique NotI site.

ES cell electroporation and generation of *langerin*$^{-/-}$ mice. 129/Sv CK35 embryonic stem (ES) cells (35) were electroporated with 30 μg of linearized targeting vector at 250 V and 500 μF of capacitance. After selection in G418 and ganciclovir, colonies were screened for homologous recombination by Southern analysis by an external probe. The 5′ single-copy probe corresponded to a 0.38-kb EcoRV-KpnI fragment isolated from a langerin genomic subclone. When tested on EcoRV-digested DNA, it hybridized either to a 7.0-kb wild-type fragment or to a 4.8-kb recombinant fragment. Positive recombinant ES clones were further validated with a 3′ external probe and with a *neo* probe to ensure that adventitious nonhomologous recombination events had not occurred in the selected clones.

Mutant ES clones were injected into BALB/c blastocysts. Male chimeras exhibiting over 60% of chimerism, as judged by coat color, were crossed with deleter transgenic mice (backcrossed on C57BL/6) to eliminate the *loxP*-flanked Neo^r cassette (58). The resulting F_1 progeny was tested for both germ line transmission and deletion of the neomycin cassette. Tails of F_1 progeny were tested by PCR with the following oligonucleotides: 5′ langerin WT, 5′-CATTT GTAGGGTGGGTGGATAGAT-3′; 3′ langerin WT, 5′-GTTTGTCCACTGT GAAGTGCGC-3′; 3′ langerin CRE, 5′-ACATTGGATATCCTCCTGTGACC T-3′. *langerin*$^{-/-}$ mice were backcrossed onto the C57BL/6 background at the Charles River facility by using a marker-assisted accelerated backcrossing program (MAX-BAX) in which nucleotide repeats (microsatellites) were used to evaluate strain-specific genomic polymorphisms to select founder animals. After three backcrosses, *langerin*$^{-/-}$ mice displayed 100% of the C57BL/6 genomic markers analyzed.

Antibodies. Anti-mouse langerin monoclonal antibodies (MAbs) were generated in-house by immunizing rats or mice with COP cells transfected with a plasmid encoding mouse langerin. MAb 929F3 (rat immunoglobulin G2a [IgG2a]) was used for langerin intracytoplasmic staining (62), and MAb 205C1 (mouse IgM) was used for cell surface staining, as it recognizes an extracellular epitope of langerin (unpublished data). These antibodies were used either uncoupled, coupled with Alexa Fluor 488 according to the manufacturer's recommendations (Molecular Probes, Eugene, Oreg.), or biotinylated. The following commercial antibodies against mouse antigens were from BD Pharmingen (San Diego, Calif.): anti-CD3 complex (clone 17A2, rat IgG2b), anti-CD4 (clone GK1.5, rat IgG2a), anti-CD8α (clone 53–6.7, rat IgG2a), anti-CD11b (clone M1/70, rat IgG2b), anti-CD11c (clone HL3, hamster IgG), anti-CD40 (clone 3/23, rat IgG2a), anti-CD80 (clone 16-10A1, hamster IgG), anti-CD86 (clone GL1, rat IgG2a), anti-*I-A*/*I-E*^{diverse} (clone 2G9, rat IgG2a), anti-*I-A*/*I-E* (clone M5/114.15.2, rat IgG2b), anti-*I-A*^{d} (clone AMS-32.1, mouse IgG2b). Control isotypes included rat IgG2a (clone R35-95), rat IgG2b (clone A95-1), Hamster IgG (clone A19-3), mouse IgM (clone G155-228). Mouse IgM and IgG2b isotype controls were from DAKO Cytometrics (Glostrup, Denmark). The fluorochromes used for flow cytometry detection were fluorescein isothiocyanate (FITC) for FL-1, R-phycoerythrin (R-PE) for FL-2, PerCP-Cy5 for FL-3, and allophycocyanin for FL-4. Secondary reagents used for flow cytometry were streptavidin-PE or streptavidin-PerCP-Cy5 when biotinylated antibodies were used. For microscopy immunostaining, secondary antibodies were goat anti-rat IgG (heavy plus light chains), goat anti-mouse IgG (heavy plus light chains), or goat anti-hamster antibody coupled with Alexa Fluor 488 or Alexa Fluor 594 (Molecular Probes).

Epidermal LC isolation. Epidermal LC were isolated by standard trypsinization (34) with porcine trypsin in Hanks' balanced salt solution (Sigma). Cells were analyzed by flow cytometry immediately after recovery or after a culture period of 3 to 4 days in RPMI 1640 medium (Life Technologies, Gaithersburg, Md.) supplemented with 10% (vol/vol) heat-inactivated fetal bovine serum (FBS; Life Technologies), 2 mM L-glutamine (Life Technologies), 5×10^{-5} M 2β-mercaptoethanol (Sigma-Aldrich), 10 mM HEPES (Life Technologies), 1 mM sodium pyruvate (Sigma), nonessential amino acids (Life Technologies), and gentamicin (40 μg/ml; Schering-Plough, Kenilworth, N.J.) supplemented with 10 ng of recombinant mouse granulocyte-macrophage colony-stimulating factor (Schering-Plough)/ml.

FITC-induced LC migration. Mice were painted on the dorsum of both ears with 25 μl of 5% FITC (Sigma) in acetone-dibutylphtalate (1/1), and the retroauricular lymph nodes (LN) were collected at the indicated time points. Cells were then isolated and labeled for flow cytometry analysis as described below.

Dendritic cell isolation and purification from lymphoid organs. Spleen, thymus, and LN were removed from CO_2-sacrificed mice. Organs were cut into small pieces, incubated at 37°C for 30 min in RPMI 1640 supplemented with 5% FBS, 10 mM HEPES, 1 mg of collagenase type IV (Sigma)/ml, and 40 μg of DNase I (Sigma)/ml. EDTA (5 mM) was added for the last 5 min. Digested fragments were filtered through a stainless steel sieve, and cell suspensions were washed twice in phosphate-buffered saline (PBS) supplemented with 5% FBS, 5 mM EDTA, and 5 μg of DNase I/ml. Spleen cell suspensions were resuspended for 3 min at room temperature in ammonium chloride to lyse red cells. Cells were then washed two more times. When required, DC were enriched in one of two ways. For FITC-induced LC migration, cells were resuspended in a PBS–1% bovine serum albumin (BSA)–5 mM EDTA buffer and magnetically separated with MACS CD11c (N418) MicroBeads (Miltenyi Biotec, Bergisch Gladbach, Germany) according to the manufacturer's instructions. Cells were then immunolabeled and analyzed by flow cytometry. For antigen presentation studies, non-DC were depleted and DC subsets were labeled and purified by fluorescence-activated cell sorting as described previously (73).

In vitro OVA presentation. Ear epidermis and dermis were separated from each other by means of the bacterial enzyme dispase II (Boehringer-Mannheim, Mannheim, Germany) at 37°C for 30 min (33). Epidermal sheets were placed floating onto complete medium. Epidermis was cultured for 72 h, whereupon cells, having migrated out from the explants, were collected, counted, and used for in vitro antigen presentation to naive T lymphocytes in the presence of different concentrations of OVA protein (grade VII; Sigma). Spleen-derived $CD8^+$ T lymphocytes from OT-I mice and $CD4^+$ T lymphocytes from OT-II mice were purified by depletion, counted, and incubated in triplicate with epidermal LC and OVA protein for 48 h in flat-bottom 96-well plates (ratio, 10^4 LC:10^5 T lymphocytes). As a positive control, stimulator cells were pulsed with 10 μM $OVA_{257–264}$ (MHC class I restricted) or 10 μM $OVA_{323–339}$ (MHC class II restricted) peptides (Neosystems, Strasbourg, France). Supernatants were collected and added to the interleukin 2 (IL-2)-dependent CTLL2 cell line. After 24 h, 1 μCi of [^{3}H]thymidine/well was added; cells were harvested after overnight incubation and radioactivity counted.

In vivo OVA presentation. Spleen cells from OT-I and OT-II mice were labeled with carboxy-fluorescein diacetate succinimidyl ester (CFSE) according to the manufacturer's instructions (Molecular Probes). C57BL/6 and *langerin*$^{-/-}$ mice were reconstituted with 50×10^6 CFSE-labeled spleen cells intravenously. Two days later, the mice were injected subcutaneously in the hind leg footpads with 50 μg of OVA protein or with PBS. Four days later, the mice were sacrificed, popliteal draining LN were collected, and T lymphocytes were stained either with CD8β or CD4. Proliferating T lymphocytes were then visualized by flow cytometry as $CFSE^+$ $CD8\beta^+$ or $CFSE^+$ $CD4^+$ events.

The procedure for evaluation of the antigen-presenting properties of splenic DC subsets has been described previously (49). Briefly, 3 mg of OVA protein was injected intravenously to *langerin*$^{-/-}$ mice and their C57BL/6 control littermates. After 18 h, spleens were collected and the two major spleen DC populations ($CD11c^+$ $CD4^+$ $CD8^-$ and $CD11c^+$ $CD4^-$ $CD8^+$) were purified by cell sorting as described previously (73). Various numbers of purified DC were then cultured with 10^4 purified naive LN $CD8^+$ T lymphocytes from OT-I mice or with 10^4

purified naive LN CD4$^+$ T lymphocytes from OT-II mice, in medium containing IL-2 to improve the sensitivity and ensure that the limiting factor is antigen presentation, not differences in the ability to induce IL-2 production. After 3 days, the cultures were pulsed for 8 h with [^{3}H]thymidine and DNA radioactivity was estimated by scintillation counting.

Immunolabeling protocol for flow cytometry. Cell surface staining was performed in PBS buffer with 1% BSA and 0.02% sodium azide. For surface and intracellular staining, the Fix&Perm kit (BD PharMingen) was used according to the manufacturer's recommendations. Antibodies were incubated for 30 min, followed by three washes. When required, second steps were done similarly. Flow cytometric analysis was performed on a FACSCalibur (BD Biosciences, Mountain View, Calif.) with CellQuest software.

Immunohistochemistry of epidermal sheets. Epidermis from ear skin was separated from the dermis by means of ammonium thiocyanate (31). Resulting sheets were fixed in acetone for 20 min at room temperature and washed in several changes of PBS and PBS containing 1% BSA and 0.02% sodium azide. They were then subjected to an immunolabeling procedure as described previously (74). Sheets were placed on a slide and mounted under coverslips with one drop of Fluoromount G (Electron Microscopy Sciences, Fort Washington, Pa.). Specimens were viewed on a Zeiss Axioscop epifluorescence microscope. Pictures were taken with an Optronics MagnaFire digital camera (Optronics, Goleta, Calif.).

Electron microscopy. Ear skin of *langerin*$^{-/-}$ mice and of their age-matched C57BL/6 littermates was fixed with Karnovsky's half-strength formaldehyde-glutaraldehyde fixative. Finely minced pieces of tissue were postfixed in 3% aqueous osmium tetroxide, followed by en bloc contrasting in Veronal-buffered 1% uranyl acetate. After dehydration in a graded series of ethanol, specimens were infiltrated and embedded in Epon 812 resin. Ultrathin sections were inspected with a Philips EM400 (Fei Company, Eindhoven, The Netherlands) at an operating voltage of 80 kV.

In vivo delivery of microorganisms. *Klebsiella pneumoniae* ATCC strain 43816, serotype 2 (American Type Culture Collection, Rockville, Md.) was grown in 100 ml of tryptic soy broth (BioMérieux, Marcy-l'Etoile, France) for 18 h at 37°C. One milliliter of the culture was added to 100 ml of fresh tryptic soy broth, grown for 2 h, washed twice in PBS at 5,000 rpm for 15 min, and resuspended in PBS to calculate the concentration by measuring the absorbance at 600 nm. Bacteria were then diluted in PBS at the desired concentration for inoculation. The inoculation dose was verified retrospectively by plating serial dilutions on tryptic soy agar plates and enumerating colonies. Mice were anesthetized with ketamine (Imalgene 500; Merial, Lyon, France). The trachea was exposed, and 50 μl of inoculum or PBS was administered. Mice were checked on a daily basis to monitor death rate and survey physical condition.

An *M. tuberculosis* H37Rv isolate was grown to mid-log phase in Middlebrook 7H9 broth (Difco) supplemented with 10% ADC enrichment (5% BSA fraction V, 2% dextrose, 0.003% beef catalase, 0.85% NaCl) and 0.05% Tween 80. Aliquots were then frozen at −80°C in the presence of 15% glycerol. Before infection, one aliquot was thawed, washed, and resuspended in PBS (pH 7.4) with 0.05% Tween 80 at 3×10^7 CFU ml^{-1}. Eight-week-old female *langerin*$^{-/-}$ and C57BL/6 control mice were infected by the aerosol route with *M. tuberculosis* H37Rv. Mice were exposed to aerosols for 15 min, which delivered approximately 200 CFU per lung. On days 1, 8, 21, and 98 postinfection, the lungs and spleen were removed aseptically and homogenized in a Potter apparatus. Serial dilutions were performed in Sauton medium and plated on solid agar Middlebrook 7H11 medium (Difco) supplemented with OADC (0.05% oleic acid, 5% BSA fraction V, 2% dextrose, 0.004% beef catalase, 0.85% NaCl). CFU were counted 14 to 21 days later. Five *langerin*$^{-/-}$ and five C57BL/6 control mice were used for each time point.

L. major strain Friedlin (*L. major* clone V1 [MHOM/IL/80/Friedlin]) amastigotes were prepared from infected Swiss *nu/nu* mice (3). Promastigotes, derived from mouse tissue amastigotes, were cultured at 26°C in HOSMEM-II medium (10) supplemented with 20% heat-inactivated fetal calf serum, 100 U of penicillin/ml, and 100 μg of streptomycin (Seromed)/ml. Infective-stage metacyclic promastigotes were isolated from stationary-phase cultures (6 day old) by negative selection with a Ficoll gradient essentially as described previously (60). One thousand metacyclic promastigotes in 10 μl of PBS were injected into the ear dermis (right ear) of *langerin*$^{-/-}$ and C57BL/6 control mice. The thickness of the ears was recorded weekly with an electronic micrometer (9).

For in vitro infection of freshly isolated epidermal LC, 2×10^7 *L. major* metacyclic promastigotes were incubated in six-well plates with 2×10^6 epidermal cells overnight at 34°C in 5% CO_2. Cells were washed, counted, and plated onto poly-L-lysine-coated coverslips for 20 min at 34°C. Coverslips were then washed, fixed in 4% paraformaldehyde for 30 min at room temperature, and washed twice. Staining was carried out at room temperature by using a biotinylated rat anti-*I-A*^{b} and a hamster polyclonal anti-*Leishmania* immune serum in PBS containing 0.05% saponin for 1 h. After three washes, coverslips were incubated with streptavidin-Alexa Fluor 488 and Texas Red anti-hamster secondary reagents for 1 h. After washes, coverslips were mounted on slides with Mowiol.

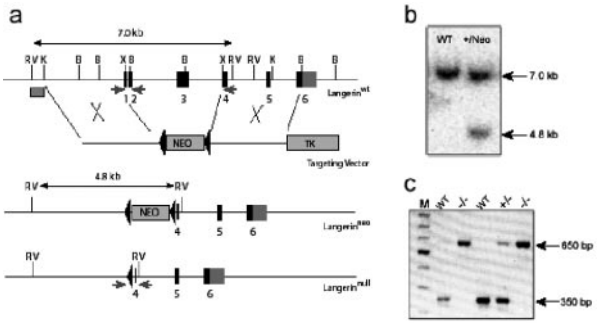

FIG. 1. Generation of the *langerin*$^{-/-}$ mouse. (a) Schematic diagram of the mouse *langerin* gene locus (Langerin^{wt}), *langerin*$^{-/-}$ targeting construct, the neomycin-containing allele (Langerin^{neo}), and the *langerin*$^{-/-}$ allele (Langerin^{null}). Filled black boxes, exons; filled dark grey box, 3′ untranslated region; filled black triangles, LoxP sequences; filled grey boxes, neomycin (NEO) and herpes simplex virus thymidine kinase (TK) expression cassettes; arrows, location of PCR oligonucleotide binding sequences; hatched black box, 5′ external EcoRV-KpnI single-copy probe. Restriction enzymes: B, BglII; E, EcoRV; K, KpnI; X, XhoI. (b) Southern blot analysis of EcoRV-digested genomic DNA from one of the injected ES clones (+/Neo) and a wild-type ES cell clone (WT). (c) PCR of genomic tail DNA from wild-type (WT), heterozygote (+/−) and *langerin*$^{-/-}$ homozygote (−/−) mice. M, 100-bp DNA ladder (Invitrogen).

Chemical carcinogenesis. For two-stage chemical skin carcinogenesis, the backs of 8-week-old mice were shaved and treated with a single application of 7,12-dimethylbenz[a]anthracene (DMBA, 25 μg in 200 μl of acetone; Sigma), followed by biweekly applications of 12-*O*-tetradecanoylphorbol-13-acetate (TPA, 200 μl of 10^{-4} M solution in acetone; Sigma) for 20 weeks. Mice were visually examined at least twice per week, and the number of mice exhibiting tumors was counted. Mice were sacrificed if moribund, if any individual tumor reached a diameter of 1 cm, or at the termination of the experiments.

RESULTS

Targeted disruption of the *langerin* gene. To characterize the role of langerin in LC, we used targeted homologous recombination to generate *langerin*$^{-/-}$ mice. To completely eliminate the expression of langerin, a targeting vector was constructed which would create a deletion in the *langerin* gene locus, spanning from 70 bp upstream of exon 1 to most of exon 4 (Fig. 1a). After electroporation and selection of CK35 ES cells, 10^3 colonies were screened by genomic Southern analysis with a 5′ external probe (Fig. 1b). Seven recombinant clones were found to have been correctly targeted, and after further verification with a 3′ external and neomycin probe (data not shown), two clones were injected into mouse blastocysts. One ES clone was found capable of germ line transmission as determined by PCR (Fig. 1c). Heterozygotes were crossed among themselves to establish a *langerin*$^{-/-}$ mouse line which demonstrated stable, Mendelian transmission of the null mutation. Three cycles of accelerated backcrosses by microsatellite-based selection were performed to generate *langerin*$^{-/-}$ mice on a C57BL/6 genetic background.

The *langerin*$^{-/-}$ mice backcrossed on the C57BL/6 background bred and developed normally. In addition, the mice did

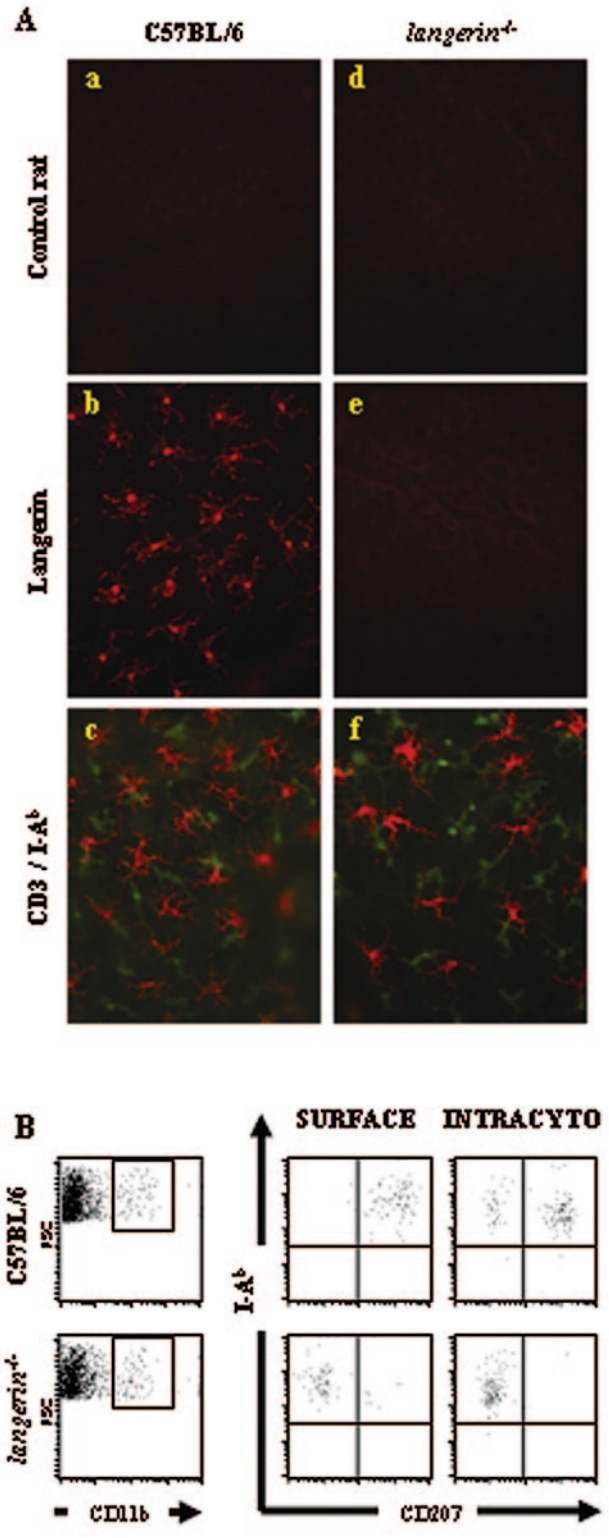

FIG. 2. Langerhans cells are present in the epidermis of *langerin*$^{-/-}$ mice. (A) Epidermal sheets from C57BL/6 control (a to c) and *langerin*$^{-/-}$ (d to f) mice fixed in acetone were stained with rat isotype antibody (a and d), rat anti-langerin MAb clone 929F3 (b and e), or hamster anti-CD3+ rat anti-*I-A*^{b} (c and f), followed by goat anti-hamster antibody–Alexa Fluor 488 (green) and goat anti-rat antibody–Alexa Fluor 594 (red). Original magnification, ×400. (B) LC were sorted from the epidermis after ear sheet trypsin treatment. Cells were stained for CD11b (PerCP-Cy5), *I-A*^{b} (PE), and cell surface (MAb 205C1 FITC) or intracellular (MAb 929F3 FITC) langerin and analyzed by flow cytometry. Cells were gated on CD11b (gate R2 in left panels) and then analyzed for *I-A*^{b} and the presence of langerin, analyzed either at the cell surface (middle panels) or intracellularly (right panels).

not present any morphological abnormalities at the macroscopic level. As expected from the targeted deletion in the *langerin* gene locus, the epidermis of the null mice completely lacked reactivity with antilangerin antibodies (Fig. 2).

We analyzed the phenotype and distribution of leukocyte populations in the spleen, thymus, and peripheral and mesenteric LN of *langerin*$^{-/-}$ mice. The qualitative and quantitative composition of DC subsets based on the expression of CD11c, CD11b, CD8α, and DEC205 was not modified compared to wild-type control mice (data not shown). No quantitative or qualitative differences were observed with respect to other cell types in lymphoid organs, i.e., B lymphocytes (CD19), T lymphocytes (CD3, CD4, CD8, TCR-αβ, and TCR-γδ), NK cells (NK1.1 and pan-NK MAb), and other non-T, non-B, non-NK leukocytes (data not shown). DC expressing langerin are notably present in the thymus, and it has been speculated that langerin could play a role in thymic T-cell selection (70). We found that the different intrathymic T-cell populations, i.e., double negative, double positive, or single positive, were present in similar percentages and absolute numbers in *langerin*$^{-/-}$ mice compared to C57BL/6 controls (data not shown). Furthermore, the *langerin*$^{-/-}$ mouse strain was crossed to both the P14 and SMARTA transgenic TCR mouse strains to assess positive selection of an MHC class I- and II-restricted TCR, respectively (36, 48). No difference was found in TCR selection in the *langerin*$^{-/-}$ mouse compared to wild-type littermates (data not shown).

Therefore, mice deficient in langerin and backcrossed on a C57BL/6 background were devoid of any remarkable alterations in their development, morphology, and leukocyte distribution in the thymus as well as secondary lymphoid organs.

MHC class II-positive DC are present in the epidermis of *langerin*$^{-/-}$ mice. Epidermal LC express high levels of langerin (70). Thus, we addressed whether this DC subset is present or altered in the epidermis of the *langerin*$^{-/-}$ mouse. Epidermal sheets from *langerin*$^{-/-}$ mice stained with an anti-MHC class II MAb showed a network of DC similar to the one observed in C57BL/6 control mice (Fig. 2A, panels c and f). Even though these cells did not express langerin, as shown by epidermal sheet staining (Fig. 2A, panel e) or immunostaining of trypsin-isolated LC (Fig. 2B), they displayed a normal dendritic morphology with normal expression of MHC class II molecules (Fig. 2A, panel f, and B). Dendritic epidermal γδ-T cells (DETC), as detected by CD3 expression, were also present in normal numbers in the *langerin*$^{-/-}$ mice (Fig. 2A, panel f).

Thus, LC are present in normal numbers in the epidermis of *langerin*$^{-/-}$ mice and display a morphology and expression of MHC class II molecules similar to that in C57BL/6 control mice.

Epidermal Langerhans cells of *langerin*$^{-/-}$ mice lack BG but otherwise do not display an altered phenotype. The cytoplasm of LC contains a unique organelle not found in other cell lineages, the BG (12). Langerin has been shown to be part of

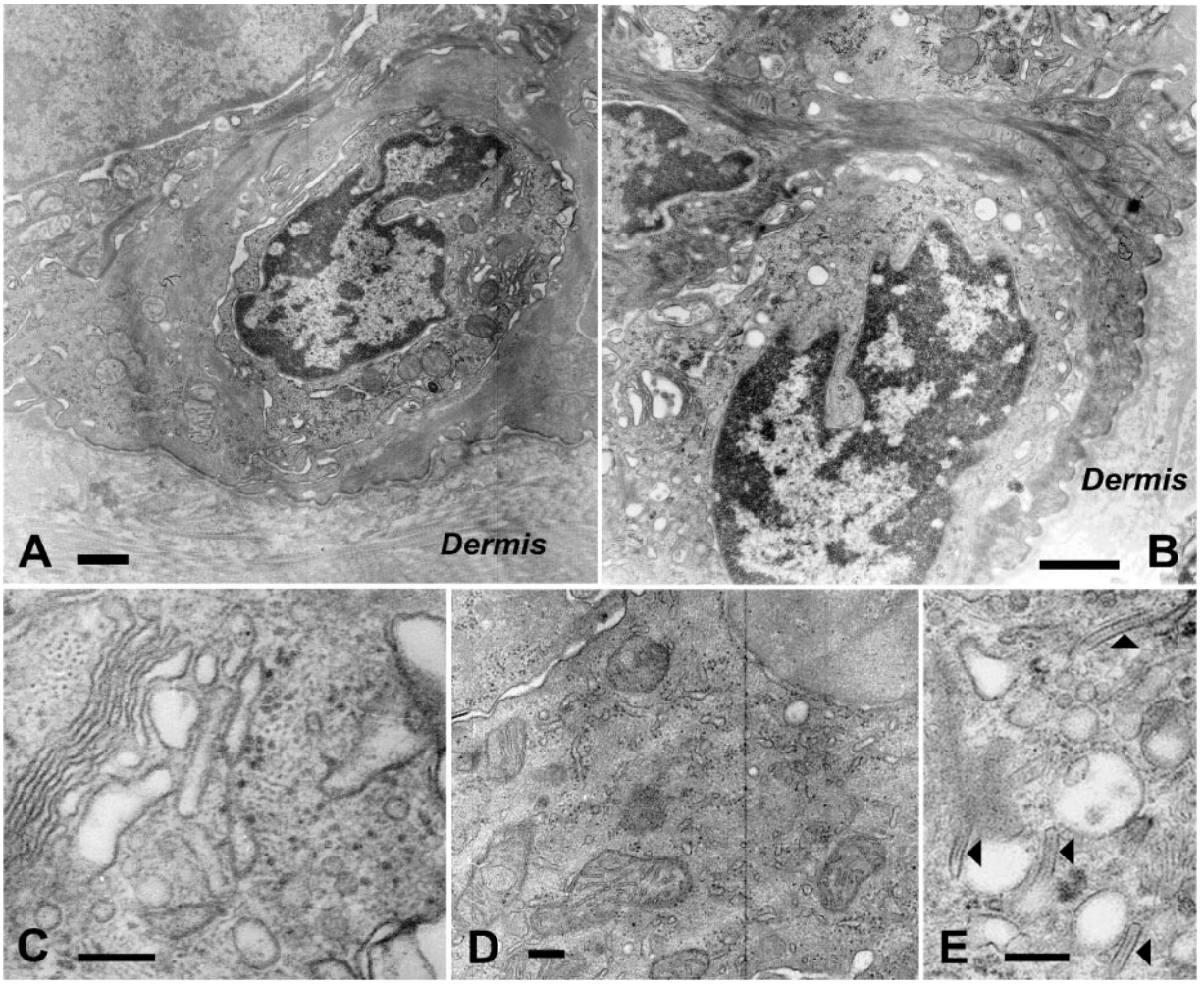

FIG. 3. Epidermal Langerhans cells in *langerin*$^{-/-}$ mice do not have BG. Native ear skin of *langerin*$^{-/-}$ mice (A, C, and D) and normal control mice (B and E) was processed for transmission electron microscopy. Rod-shaped BG were readily detected in LC from normal mice (panel B, lower left region enlarged in panel E; BG are marked with arrowheads). In the epidermis of *langerin*$^{-/-}$ mice, none of the inspected LC possessed BG. Two high-power examples from two different cells are given in panels C and D. Magnifications and bars: A, ×7,000 and 1 μm; B, ×9,800 and 1 μm; C, ×51,000 and 200 nm; D, ×25,000 and 200 nm; E, ×40,000 and 200 nm.

these organelles and to induce their formation (72). Inspection of ultrathin sections of the epidermis from normal mice readily revealed the presence of unequivocal BG in virtually every LC at first glance (Fig. 3B and E). The BG occurred sometimes in the shape of tennis rackets but more often as rods. In the skin of *langerin*$^{-/-}$ mice, long stretches of epidermis were examined. In 22 unequivocally identified LC (some of which were examined two or three times on serial sections) and on numerous small profiles of LC dendrites, we were unable to detect any BG at all (Fig. 3A, C, and D). DETC could readily be distinguished from LC by their characteristic electron-dense round granules (54).

LC from ear epidermis of C57BL/6 and *langerin*$^{-/-}$ mice were isolated after trypsin treatment. The phenotype of these freshly isolated LC was identical for both mouse lines with high expression of MHC class II, CD11c, CD11b (Fig. 2B), DEC-205, and E-cadherin (data not shown) but no detectable CD8α, CD40, or CD86 (data not shown). When cultured for a few days in the presence of granulocyte-macrophage colony-stimulating factor, LC from both *langerin*$^{-/-}$ and wild-type mice matured and became activated, expressing CD40, CD80, and CD86 (data not shown).

In summary, our results show that langerin is essential for BG formation, i.e., that no other gene can substitute for this function, but that LC from *langerin*$^{-/-}$ mice otherwise display an identical phenotype to that of wild-type control littermates.

Antigen capture and migration of epidermal Langerhans cells is not altered in *langerin*$^{-/-}$ mice. Due to their physical location, LC are sentinels for contact with microbial or environmental antigens. They capture and process exogenous material and subsequently migrate into skin draining LN to present antigen to specific T lymphocytes. We thus studied whether these functions would be affected by the absence of langerin.

In vitro, freshly isolated LC from *langerin*$^{-/-}$ epidermis were able to phagocytose zymosan particles as efficiently as LC from wild-type mice (data not shown). Furthermore, LC were able to crawl out from dispase-treated epidermis of *langerin*$^{-/-}$

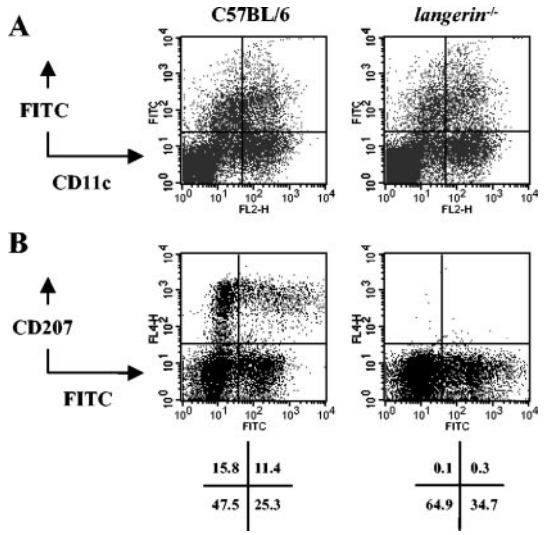

FIG. 4. In vivo migration of epidermal Langerhans cells is unaffected in *langerin*$^{-/-}$ mice painted with FITC. C57BL/6 controls and *langerin*$^{-/-}$ mice were painted with FITC on the dorsa of both ears. Two days later, mice were sacrificed and cells from draining LN were harvested, enriched for CD11c-expressing cells with magnetic beads, and immunolabeled for flow cytometry analysis. (A) Dot plots show FITC versus CD11c from the LN draining the FITC-painted ears of both mouse lines; (B) langerin/CD207 versus FITC dot plots on CD11c^{+}-gated LN cells stained for intracellular langerin. Percentages for each quadrant are noted.

mice (33), indicating that the ex vivo spontaneous migratory capacity of these cells is not impaired. Similar to their wild-type counterparts, the crawl out cells from *langerin*$^{-/-}$ mice also expressed high levels of MHC class II molecules as well as the activation markers CD40, CD80, and CD86 (data not shown). Furthermore, their morphology under phase-contrast microscopy (cytoplasmic processes, veils) and under the hemocytometer (hairy appearance) was indistinguishable from control LC.

To assess whether antigen capture and the migratory capability of LC are modified in vivo in *langerin*$^{-/-}$ mice, FITC was applied onto the ears as a tracer. The retroauricular draining LN were subsequently collected and monitored for the presence of FITC. We observed cell-associated FITC in the draining LN both in *langerin*$^{-/-}$ and wild-type control mice from day 1 up to day 4, with a peak on day 2. FITC was carried into the draining LN by CD11c^{+} as well as by CD11c^{-} cells (Fig. 4A). The FITC-positive CD11c^{+} cells were CD8α^{-} but CD11b^{int}, CD40^{+}, CD80^{+}, and CD86^{+} (data not shown). In the C57BL/6 control mice, we found FITC associated with cells expressing langerin (Fig. 4B) and activation markers (data not shown). In peripheral LN, LC constitute a substantial fraction of the CD11c^{+} CD8α^{-} subset. In *langerin*$^{-/-}$ mice, the LC cannot be identified de facto with langerin-specific MAb. However, the proportion of FITC-positive CD11c^{+} cells in the draining LN of C57BL/6 and *langerin*$^{-/-}$ mice was similar (about 35% of the CD11c^{+} cells) (Fig. 4B), inferring that LC are able to capture FITC and migrate into draining LN, regardless of the presence of the langerin molecule.

Together, our data demonstrate that antigen capture and migration properties of epidermal LC are unaffected by the absence of langerin.

Processing and presentation of exogenous protein antigen is not impaired in *langerin*$^{-/-}$ mice. Since lack of langerin hampered neither antigen capture nor the migratory capability of LC, we investigated next whether langerin plays a role in the processing of a model antigenic protein (OVA) and the subsequent presentation of derived peptides to specific T lymphocytes in the context of MHC class I and II molecules.

LC that had crawled out of the epidermis were harvested, mixed with purified OVA-specific naive T lymphocytes from OT-I or OT-II mice, and cultured in the presence of different concentrations of OVA protein. Results depicted in Fig. 5A indicate that *langerin*$^{-/-}$ LC were able to process OVA protein and to present peptides on MHC class I and II molecules. Moreover, no difference was observed when compared with LC derived from C57BL/6 control mice (Fig. 5A).

To test the capacity of the DC to capture, process, and present OVA in vivo, we adoptively transferred OT-I or OT-II spleen cells previously labeled with CFSE to C57BL/6 and *langerin*$^{-/-}$ mice. Forty-eight hours later, we injected soluble OVA protein into the footpads of the reconstituted mice. Four days later, the draining LN were harvested and CFSE fluorescence was analyzed as a marker of OVA-reactive T-lymphocyte divisions. As shown in Fig. 5B, both CD8^{+} (OT-I) and CD4^{+} (OT-II) OVA-specific T lymphocytes had divided in vivo, and no difference in T-lymphocyte proliferation was detected between C57BL/6 and *langerin*$^{-/-}$ mice.

Langerin has been previously described in spleen CD8α^{+} DC (39). Furthermore, it is known that the CD8α^{+} DC subset in the spleen is responsible for cross-presentation of exogenous OVA to MHC class I-restricted T lymphocytes (20, 49). To investigate whether lack of langerin affects cross-presentation by CD8α^{+} DC, we injected soluble OVA protein intravenously and collected spleens 18 h later. Spleen DC were then enriched and sorted into CD8α^{+} and CD4^{+} subpopulations. Each of these populations was cultured for 3 days with OVA-specific T lymphocytes from either OT-I or OT-II mice in the presence of exogenous IL-2. The response of OT-II T lymphocytes assesses the immunostimulating features of DC displaying OVA peptides bound to MHC class II *I-A*^{b} while the response of OT-I T lymphocytes assesses the immunostimulating features of DC displaying OVA peptides bound to MHC class I *H-2K*^{b} as a result of cross-presentation. As depicted in Fig. 5C, there was no difference in cross-presentation between the *langerin*$^{-/-}$ mice and the controls. Thus, the CD8α^{+} DC of the *langerin*$^{-/-}$ mice do retain their cross-presentation capacity to OT-I cells. Furthermore, the CD4^{+} spleen DC is the major population subset presenting OVA to the OT-II T lymphocytes in both mouse lines. A series of culture experiments with soluble and cell-bound OVA confirmed this result (data not shown).

Our data thus indicate that lack of langerin does not influence protein antigen processing and presentation, as evaluated either in vitro or in vivo.

***langerin*$^{-/-}$ mice do not display altered susceptibility to pathogenic microorganisms.** Langerin is an endocytic receptor of the C-type lectin family, with specificity for mannose, GlcNac, and fucose residues (61, 72). Langerin-expressing cells are found in the epidermis and in epithelia of pluristratified mucosa, such as in the respiratory tract. Previous observations (70; unpublished data) have validated the presence of langerin in airway epithelium. Based on these considerations, we inocu-

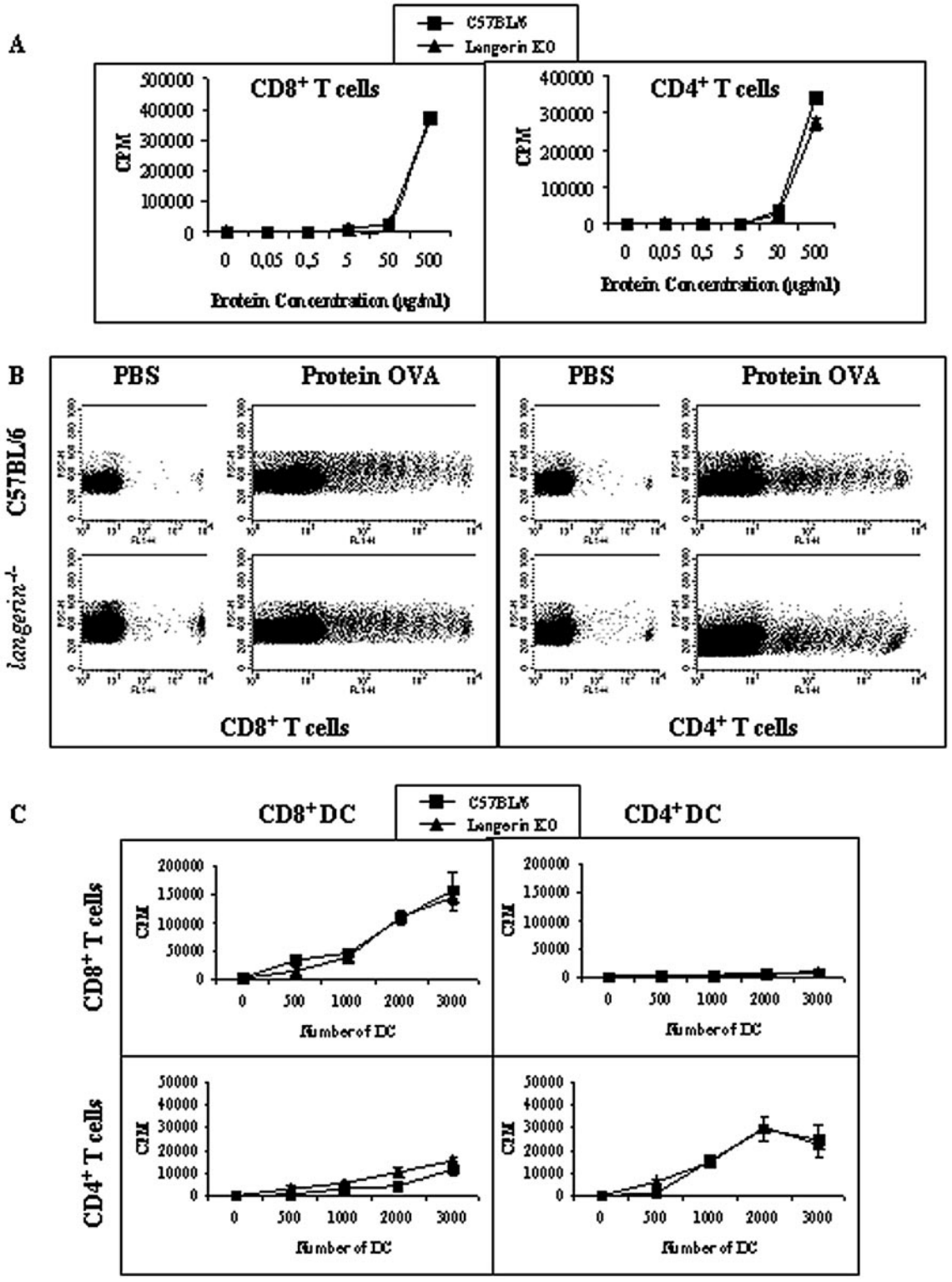

FIG. 5. Protein antigen presentation and cross-presentation is not altered in *langerin*$^{-/-}$ mice. (A) In vitro OVA presentation. Langerhans cells were allowed to crawl out from the epidermis of C57BL/6 control and *langerin*$^{-/-}$ mice. After 72 h, cells were counted and placed in 96-well plates with different concentrations of OVA protein and OVA-specific CD8$^+$ T lymphocytes from OT-I (MHC class I restricted) or CD4$^+$ T lymphocytes from OT-II (MHC class II restricted) mice for 48 h. Triplicate supernatants were collected and added to the IL-2-dependent CTLL2 cell line, and proliferation was assessed with [^{3}H]thymidine. (B) In vivo OVA presentation. C57BL/6 control and *langerin*$^{-/-}$ mice were reconstituted with CFSE-labeled spleen cells from OT-I or OT-II mice. After 48 h, the recipient mice were injected with OVA protein or PBS in the footpads. Four days later, draining LN cells were harvested and analyzed for CFSE staining by flow cytometry to assess the specific proliferation of the adoptively transferred T lymphocytes. (C) OVA cross-presentation. C57BL/6 and *langerin*$^{-/-}$ mice were injected intravenously with OVA protein and sacrificed 18 h later for spleen recovery. DC were enriched from spleens, and CD8$^+$ or CD4$^+$ subpopulations were sorted. Graded numbers of each DC subpopulation were then cultured in duplicate for 3 days with 10,000 OVA-specific T lymphocytes from OT-I or OT-II mice. Each well was pulsed with [^{3}H]thymidine for 8 h, and the incorporated radioactivity was counted.

lated *langerin*$^{-/-}$ and C57BL/6 mice with different pathogenic microorganisms to assess differences in susceptibility.

Klebsiellae are enterobacteria that normally produce prominent polysaccharide capsules with mannose residues (5). Cell wall-associated mannoproteins have been described for *Candida albicans* and are implicated in immunogenicity (15, 32). We inoculated *langerin*$^{-/-}$ and wild-type control mice with *K. pneumoniae* (10^3 CFU) and *C. albicans* (10^6 CFU) by intratracheal delivery. Mice were monitored every day for survival, and our results indicate that both mouse lines displayed a similar death rate in response to either *K. pneumoniae* (Fig. 6A) or *C. albicans* (data not shown).

Given the diversity of the polymannosylated constituents of the envelope of mycobacteria (22) and the description that DC play a role in mycobacterial infection (19), we analyzed whether a lack of langerin influences susceptibility to *M. tuberculosis*. Thus, 200 CFU of *M. tuberculosis* H37Rv was delivered to mice by aerosol. The *M. tuberculosis* load in the spleen and lungs was then monitored at different time points. As shown in Fig. 6B, *M. tuberculosis* developed within the tissues of mice of both lines with similar kinetics and multiplication rates. As expected from the natural route of delivery, live bacilli were recovered from lungs at all time points and were detected in the spleen 21 days after aerosol delivery, which corresponds to a hematogenous spread of *M. tuberculosis*. Thus, langerin does not play a dominant role in *M. tuberculosis* uptake in the airway tract or in dissemination of the bacillus in distant mouse tissues.

Leishmania are protozoan parasites, transmitted to mammalian hosts by small blood-feeding female insects known as sand flies, such as *Phlebotomus papatasi* for *L. major*. Due to their physical location, LC may play a particular role in the early processes following dermal delivery of metacyclic promastigotes, which represent the infective developmental stage of the parasite (6). We delivered 1,000 *L. major* metacyclic promastigotes intradermally in the right ears (ventral side) of *langerin*$^{-/-}$ and wild-type control mice. Every week, the thickness of both ears was measured, with the left ears being the controls. As shown in Fig. 6C, we observed ear swelling in both mouse lines, with similar kinetics and size. As expected from previous reports, the ear thickness of C57BL/6 mice went back to a normal shape and size, and the same result was observed for *langerin*$^{-/-}$ mice. When 10^3 *L. major* promastigotes were delivered intradermally to the cured mice in the opposite ears, no swelling was observed in either of the two mouse lines (data not shown). Finally, in vitro, LC isolated from ears of *langerin*$^{-/-}$ mice were able to phagocytose the parasites as efficiently as their C57BL/6 counterparts (Fig. 6C).

Taken together, we did not observe any differences between *langerin*$^{-/-}$ and C57BL/6 mice in response to the microorganisms we studied. *langerin*$^{-/-}$ and control mice died at a similar rate when infected with *K. pneumoniae* and *C. albicans*. In addition, *M. tuberculosis* proliferated to the same extent in the organs of both mouse lines, and intradermal inoculation of a low dose of *L. major* metacyclic promastigotes led to an identical phenotype, namely the development of a transient cutaneous lesion that heals, as well as the absence of a lesion at a second site of delivery, i.e., the development of so-called resistance to a second inoculum.

Chemically induced skin carcinogenesis is not affected in *langerin*$^{-/-}$ mice. To test whether langerin is involved in the development of an experimental skin tumor, C57BL/6 and *langerin*$^{-/-}$ mice were exposed to a two-stage chemical carcinogenesis protocol. First, mice received a single skin application of the carcinogen DMBA, and then biweekly, TPA was applied as a tumor promoter. Mice were visually examined twice a week, and the number of mice exhibiting tumors was counted. This carcinogenesis protocol leads directly to the development of predominantly squamous cell carcinomas. As shown in Fig. 7, the kinetics of tumor development in *langerin*$^{-/-}$ mice was similar to that of C57BL/6 control mice. Moreover, the number of tumors per mouse was not different between the two mouse lines (2 to 3 per mouse) (data not shown). It is known that the protocol used in our study entails tumor initiation in epidermal keratinocytes with the oncogenic activation of the c-Ha-*ras* gene (50). Taken together, these results indicate that langerin-dependent functions of LC do not affect *ras*-mediated keratinocyte oncogenic processes in vivo.

DISCUSSION

Langerin is a transmembrane type II Ca^{2+}-dependent lectin with a single carbohydrate recognition domain displaying specificity for mannose, *N*-acetyl-glucosamine, and fucose (61, 72). Langerin is an endocytic receptor that translocates ligands from the cell surface into BG. To get further insight into the role of langerin in LC functions, we performed targeted disruption of the *langerin* gene. The resulting *langerin*$^{-/-}$ mouse was backcrossed on a C57BL/6 background. These mice developed and bred normally. An epidermal MHC class II^{high} dendritic network was observed in *langerin*$^{-/-}$ mice, indistinguishable from that of C57BL/6 control mice. Our results indicate that langerin is not necessary for the establishment of the LC system in the epidermis and support a recent description that, even though some MHC class II-positive cells are present in the epidermis of newborn mice, langerin expression is detectable only 2 to 3 days after birth (67). The phenotype of freshly isolated epidermal LC from *langerin*$^{-/-}$ mice was further identical to that of C57BL/6 controls, including expression of the type I lectin DEC205/CD205 and E-cadherin. Other leukocyte cell populations such as DETC or dermal DC were also normally detected in *langerin*$^{-/-}$ skin. Thus, absence of langerin does not perturb the development of leukocytes known to display immune functions in the skin. In this context, the development of LC is abolished in *tgfb1*$^{-/-}$ mice (14) or in *id2*$^{-/-}$ mice (26), with Id2 being a transcription factor induced by transforming growth factor β1. Notably, even though the skin of these mice is totally devoid of LC, no defect has yet been reported in immune responses against pathogenic microorganisms.

A major feature of the *langerin*$^{-/-}$ mouse was the absence of BG in the LC. Transfection of fibroblasts with langerin cDNA is known to induce the formation of BG (72). Our present data demonstrate that langerin is essential for this function, i.e., that no molecular redundancy exists for inducing the development of BG. BG have been described as a component of the endocytic pathway (28, 66) and implicated in the processing of antigenic molecules (63). Langerin is internalized into BG

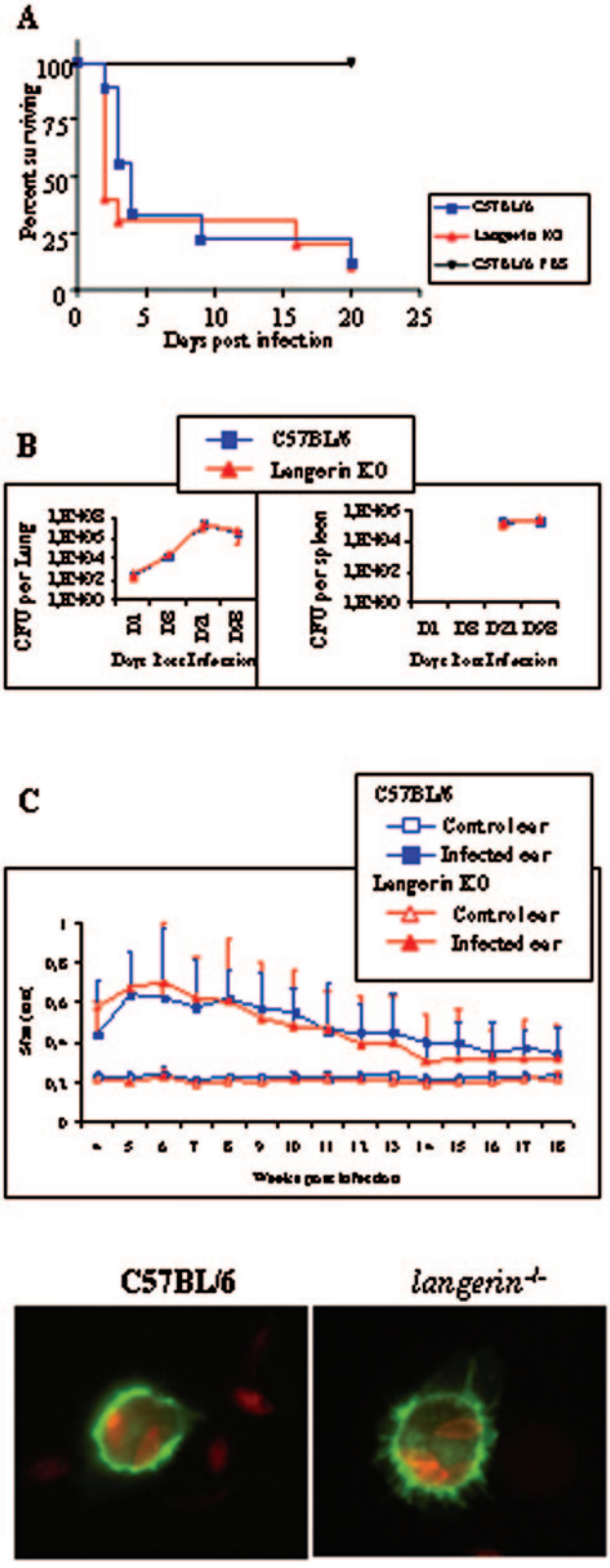

FIG. 6. *langerin*$^{-/-}$ and C57BL/6 mice are equally susceptible to pathogenic microorganisms. (A) *K. pneumoniae. K. pneumoniae* (10^3 CFU) or PBS was delivered directly into the tracheas of anesthetized C57BL/6 control and *langerin*$^{-/-}$ mice. The survival curves are presented. (B) *M. tuberculosis*. C57BL/6 control and *langerin*$^{-/-}$ mice were exposed to *M. tuberculosis*-loaded aerosols. Five mice per group were sacrificed on days 1, 8, 21, and 98. Spleens and lungs were homogenized, and *M. tuberculosis* CFU were counted after culture on solid medium. Mean CFU ± standard deviations are represented. (C) *L. major*. *L. major* metacyclic promastigotes (10^3) were delivered intradermally into the right ear of C57BL/6 control and *langerin*$^{-/-}$ mice (ventral side). The thickness of both ears was recorded weekly and plotted ± standard deviation. Pictures show that epidermally isolated LC from both *langerin*$^{-/-}$ and C57BL/6 control mice were able to capture parasites. Cells (2×10^6) were cultured at 34°C in 5% CO_2 overnight with 2×10^7 *L. major* promastigotes. After adhesion to poly-L-lysine-coated coverslips and fixation, cells were stained with an anti-*I-A*^{b} biotinylated MAb and *L. major* was stained with a hamster polyclonal immune serum. Primary antibodies were detected with streptavidin-Alexa Fluor 488 (green) and anti-hamster antibody–Texas Red (red). Original magnification, ×1,000.

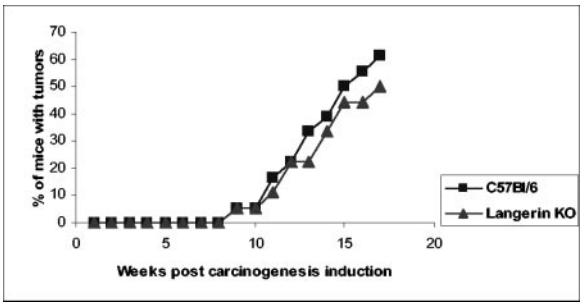

FIG. 7. Chemical skin carcinogenesis is not modified in *langerin*$^{-/-}$ mice. C57BL/6 control and *langerin*$^{-/-}$ mice were subjected to a two-stage chemical carcinogenesis protocol with DMBA as the initiator and TPA as the promoter. Skin tumors were counted biweekly, and the graph represents the percentage of mice bearing tumors.

when cross-linked by an antibody (72). It is likely that BG represent membrane domains of tubular recycling endosomes where langerin accumulates (38). Langerin belongs to a family of lectin receptors that capture carbohydrate-bearing molecules (23). Interestingly, in human LC, the subcellular routing of langerin largely overlaps with that of CD1a (27, 57), a molecule related to MHC class I products and implicated in the presentation of antigenic lipids and glycolipids (45). A recent study has shown that human langerin and CD1a interact for the uptake and presentation of glycolipids derived from *Mycobacterium leprae*, resulting in the induction of a cellular immune response (30, 41). However, a parallel between human and mouse LC is not obvious at this level. Thus, group I CD1 molecules (CD1a, CD1b, and CD1c) are notoriously absent in mice (18), which only express the group II CD1 molecule CD1d, with an intracellular routing quite different from that of human CD1a. Indeed, mouse CD1d traffics deeper into late lysosomes in a pattern that resembles human CD1b (18, 64), thus not suggestive of a routing into BG.

Despite the lack of BG, we were not able to show any significant functional differences between *langerin*$^{-/-}$ mice and their wild-type littermates. The migration of LC to skin draining LN was not impaired in *langerin*$^{-/-}$ mice, implying that the absence of BG formation does not perturb this function. Furthermore, OVA protein was processed and the derived peptides presented to CD4-positive and CD8-positive T lymphocytes with normal efficiency in *langerin*$^{-/-}$ mice. Exogenous antigens are normally processed and presented by MHC class

II molecules to $CD4^+$ T lymphocytes, whereas antigens presented on MHC class I molecules are generally of endogenous origin. However, exogenous antigens can enter the MHC class I presentation pathway in professional antigen-presenting cells and, thereby, prime $CD8^+$ T lymphocytes, a process termed cross-presentation. This has been originally described for cell-associated antigens (11, 16) as well as for soluble antigens (46). It has been shown that splenic $CD8\alpha^+$ DC are responsible for the cross-presentation of exogenous antigens to $CD8^+$ T lymphocytes (49). Interestingly, although langerin is expressed exclusively by the $CD8\alpha^+$ DC subset in the mouse spleen (39), our results show that cross-presentation of soluble OVA by splenic $CD8\alpha^+$ DC was not affected in *langerin*$^{-/-}$ mice.

Immature DC, including LC, are leukocytes that recognize surface molecules displayed by microorganisms or the soluble components they release. They capture and internalize bound microorganisms or microbial molecules through several mechanisms, including endocytosis following lectin-mediated recognition of sugar patterns displayed by the microorganisms (23). In this context, human langerin has been shown to bind mannosylated gp120 from human immunodeficiency virus (68) and was recently reported to capture glycolipids derived from *M. leprae* (30). We thus tested the susceptibility of *langerin*$^{-/-}$ mice to the live mannosylated pathogenic microorganisms *K. pneumoniae*, *C. albicans*, and *M. tuberculosis*, administered to reach the airway epithelium expressing langerin (70; our unpublished data). *K. pneumoniae* is the most common gram-negative pathogen causing community-acquired bacterial pneumonia (17), and is involved in the outbreak of nosocomial infections, mainly in immunocompromised individuals (56). *C. albicans* is a dimorphic, opportunistic fungal pathogen that is responsible for the majority of fungal infections in immunocompromised hosts. DC are able to interact with *C. albicans* and to discriminate between virulent and nonvirulent forms of the fungus (21). Although DC are not the primary targets for infection by mycobacteria, they play a role in modulating the cellular immune response induced by the bacilli (47). Thus, the control of *M. tuberculosis* infection requires a coordinated interaction of macrophages, DC, and T lymphocytes acting as essential effectors (24). The lectin DC-SIGN is a receptor for *M. tuberculosis* (25, 65). It has been suggested that after binding of mannosylated components of the *M. tuberculosis* envelope, DC-$SIGN^+$ DC from the respiratory tract may transport bacilli to the draining LN and thus contribute to chronic infection (65). Since langerin and DC-SIGN share similar carbohydrate specificity, we reasoned that pulmonary LC may also play an important role in early steps of infection in mice by means of *M. tuberculosis* capture by langerin. However, *langerin*$^{-/-}$ mice reacted similarly to C57BL/6 controls to each of the pathogenic microorganisms we tested. These findings could suggest that other LC molecules may compensate for lack of langerin. Alternatively, DC in the lamina propria of the airway epithelium may play a dominant role in shaping the response to these pathogens.

Mice were also inoculated intradermally with *L. major*, a parasite displaying skin tropism. In their natural habitat, the parasites are inoculated by a sand fly during blood feeding in the ears of rodents. Even though *Leishmania* have been essentially described to be routed into phagolysosomes of macrophages, it is clear from recent studies that DC also play an important role in shaping the immune response (6, 51, 52, 59, 69). LC in the epidermis are potential candidates for parasite phagocytosis, and we speculated that langerin could be involved in this process and/or in the subsequent development of the parasitic processes, whether those are clinically silent or assessed by transient cutaneous lesions. Indeed, it has been described that *Leishmania* can be taken up by LC in vitro and in vivo (13) and that they play a role in parasite transport and initiation of the immune response against *L. major* (42, 43), at least after subcutaneous delivery of very high numbers of stationary-phase promastigotes. We observed that both the *langerin*$^{-/-}$ and C57BL/6 mouse lines developed reversible cutaneous lesions, indicating that langerin does not play a dominant role in this process. We also observed that LC from both mouse lines were able to phagocytose *L. major* in vitro. It should again be noted that LC express numerous cell surface receptors, and lack of langerin could be overcome by alternative receptors. In addition, recent contradictory reports have been published regarding the cells that shuttle the parasite into draining LN after skin infection (6, 52). Finally, it is well known that C57BL/6 mice are resistant to *L. major* (55). In this context, our results do not exclude that infection of *langerin*$^{-/-}$ mice on a susceptible background (e.g., BALB/c) may reveal a role for langerin not seen on the present C57BL/6 background.

Overall, our data show that the absence of mouse langerin does not lead to any phenotypical, morphological, or functional perturbations in vivo and in the ex vivo systems studied here. These observations are interestingly corroborated by a study reported by Mommaas and colleagues who described a human case of epidermal LC lacking BG (44). The BG-negative individual did not show any signs of pathology. Furthermore, LC were present in normal numbers and morphology and displayed a normal antigen-presenting capacity. Thus, the absence of langerin, and consequently, that of BG, does not yet reveal the role of this molecule and the resulting organelles in the shaping of the immune response by LC. In this context, a study with herpes simplex virus has recently reconsidered the potential role of LC in in vivo T-cell priming (1), suggesting that LC may play a carrier or shuttle function, but are not the key antigen-presenting cells for induction of an immune response. However, other reports have here described a role for LC, such as in infection with Dengue virus (76) or encephalitis virus (37). Even though it is known which carbohydrates bind to langerin (61), the range of its biological ligand(s) is still not known. Other lectins are expressed by LC, including DEC205, and redundancy for the capture of pathogens bearing carbohydrate residues cannot be excluded. Further studies involving double-deficient mice, such as langerin-DEC205 knockoouts, could help to unravel unique functions of LC. The *langerin*$^{-/-}$ mouse line should represent a valuable tool for further investigation of the function of langerin and BG and, by extension, the role of LC in particular models that have not been addressed in the present study.

ACKNOWLEDGMENTS

We thank A. Gillet and M. Malissen (CIML) for advice, S. Richelme for blastocyst injections, Maï Lebastard (Institut Pasteur) for technical help with *Leishmania*, and Cyril Desvignes, Patrick Hardy, and François Veillette (Charles River) for *Klebsiella* and *Candida* experiments. We are grateful to C. Peronne (Schering-Plough) for PCR genotyping.

This study was supported in part by INSERM, Institut Pasteur, and CNRS (including Appel d'offres Puce à ADN du CNRS).

REFERENCES

1. **Allan, R. S., C. M. Smith, G. T. Belz, A. L. van Lint, L. M. Wakim, W. R. Heath, and F. R. Carbone.** 2003. Epidermal viral immunity induced by CD8alpha+ dendritic cells but not by Langerhans cells. Science **301:**1925–1928.
2. **Anjuere, F., G. M. del Hoyo, P. Martin, and C. Ardavin.** 2000. Langerhans cells develop from a lymphoid-committed precursor. Blood **96:**1633–1637.
3. **Antoine, J. C., C. Jouanne, and A. Ryter.** 1989. Megasomes as the targets of leucine methyl ester in Leishmania amazonensis amastigotes. Parasitology **99**(Pt. 1)**:**1–9.
4. **Ardavin, C., G. Martinez del Hoyo, P. Martin, F. Anjuere, C. F. Arias, A. R. Marin, S. Ruiz, V. Parrillas, and H. Hernandez.** 2001. Origin and differentiation of dendritic cells. Trends Immunol. **22:**691–700.
5. **Athamna, A., I. Ofek, Y. Keisari, S. Markowitz, G. G. Dutton, and N. Sharon.** 1991. Lectinophagocytosis of encapsulated *Klebsiella pneumoniae* mediated by surface lectins of guinea pig alveolar macrophages and human monocyte-derived macrophages. Infect. Immun. **59:**1673–1682.
6. **Baldwin, T., S. Henri, J. Curtis, M. O'Keeffe, D. Vremec, K. Shortman, and E. Handman.** 2004. Dendritic cell populations in *Leishmania major*-infected skin and draining lymph nodes. Infect. Immun. **72:**1991–2001.
7. **Banchereau, J., and R. M. Steinman.** 1998. Dendritic cells and the control of immunity. Nature **392:**245–252.
8. **Barnden, M. J., J. Allison, W. R. Heath, and F. R. Carbone.** 1998. Defective TCR expression in transgenic mice constructed using cDNA-based alpha- and beta-chain genes under the control of heterologous regulatory elements. Immunol. Cell Biol. **76:**34–40.
9. **Belkaid, Y., S. Mendez, R. Lira, N. Kadambi, G. Milon, and D. Sacks.** 2000. A natural model of Leishmania major infection reveals a prolonged "silent" phase of parasite amplification in the skin before the onset of lesion formation and immunity. J. Immunol. **165:**969–977.
10. **Berens, R. L., and J. J. Marr.** 1978. An easily prepared defined medium for cultivation of Leishmania donovani promastigotes. J. Parasitol. **64:**160.
11. **Bevan, M. J.** 1976. Minor H antigens introduced on H-2 different stimulating cells cross-react at the cytotoxic T cell level during in vivo priming. J. Immunol. **117:**2233–2238.
12. **Birbeck, M. S., A. S. Breathnach, and J. D. Everall.** 1961. An electron microscope study of basal melanocytes and high-level clear cells (Langerhans cells) in vitiligo. J. Investig. Dermatol. **37:**51.
13. **Blank, C., H. Fuchs, K. Rappersberger, M. Rollinghoff, and H. Moll.** 1993. Parasitism of epidermal Langerhans cells in experimental cutaneous leishmaniasis with Leishmania major. J. Infect. Dis. **167:**418–425.
14. **Borkowski, T. A., J. J. Letterio, A. G. Farr, and M. C. Udey.** 1996. A role for endogenous transforming growth factor beta 1 in Langerhans cell biology: the skin of transforming growth factor beta 1 null mice is devoid of epidermal Langerhans cells. J. Exp. Med. **184:**2417–2422.
15. **Calderone, R., R. Diamond, J. M. Senet, J. Warmington, S. Filler, and J. E. Edwards.** 1994. Host cell-fungal cell interactions. J. Med. Vet. Mycol. **32**(Suppl. 1)**:**151–168.
16. **Carbone, F. R., and M. J. Bevan.** 1990. Class I-restricted processing and presentation of exogenous cell-associated antigen in vivo. J. Exp. Med. **171:**377–387.
17. **Carpenter, J. L.** 1990. Klebsiella pulmonary infections: occurrence at one medical center and review. Rev. Infect. Dis. **12:**672–682.
18. **Dascher, C. C., and M. B. Brenner.** 2003. Evolutionary constraints on CD1 structure: insights from comparative genomic analysis. Trends Immunol. **24:**412–418.
19. **Demangel, C., A. G. Bean, E. Martin, C. G. Feng, A. T. Kamath, and W. J. Britton.** 1999. Protection against aerosol Mycobacterium tuberculosis infection using Mycobacterium bovis Bacillus Calmette Guerin-infected dendritic cells. Eur. J. Immunol. **29:**1972–1979.
20. **den Haan, J. M., S. M. Lehar, and M. J. Bevan.** 2000. CD8(+) but not CD8(-) dendritic cells cross-prime cytotoxic T cells in vivo. J. Exp. Med. **192:**1685–1696.
21. **d'Ostiani, C. F., G. Del Sero, A. Bacci, C. Montagnoli, A. Spreca, A. Mencacci, P. Ricciardi-Castagnoli, and L. Romani.** 2000. Dendritic cells discriminate between yeasts and hyphae of the fungus Candida albicans. Implications for initiation of T helper cell immunity in vitro and in vivo. J. Exp. Med. **191:**1661–1674.
22. **Ehlers, M. R., and M. Daffe.** 1998. Interactions between Mycobacterium tuberculosis and host cells: are mycobacterial sugars the key? Trends Microbiol. **6:**328–335.
23. **Figdor, C. G., Y. van Kooyk, and G. J. Adema.** 2002. C-type lectin receptors on dendritic cells and Langerhans cells. Nat. Rev. Immunol. **2:**77–84.
24. **Flynn, J. L., and J. D. Ernst.** 2000. Immune responses in tuberculosis. Curr. Opin. Immunol. **12:**432–436.
25. **Geijtenbeek, T. B., S. J. Van Vliet, E. A. Koppel, M. Sanchez-Hernandez, C. M. Vandenbroucke-Grauls, B. Appelmelk, and Y. Van Kooyk.** 2003. Mycobacteria target DC-SIGN to suppress dendritic cell function. J. Exp. Med. **197:**7–17.
26. **Hacker, C., R. D. Kirsch, X. S. Ju, T. Hieronymus, T. C. Gust, C. Kuhl, T. Jorgas, S. M. Kurz, S. Rose-John, Y. Yokota, and M. Zenke.** 2003. Transcriptional profiling identifies Id2 function in dendritic cell development. Nat. Immunol. **4:**380–386.
27. **Hanau, D., M. Fabre, D. A. Schmitt, J. C. Garaud, G. Pauly, M. M. Tongio, S. Mayer, and J. P. Cazenave.** 1987. Human epidermal Langerhans cells cointernalize by receptor-mediated endocytosis "nonclassical" major histocompatibility complex class I molecules (T6 antigens) and class II molecules (HLA-DR antigens). Proc. Natl. Acad. Sci. USA **84:**2901–2905.
28. **Hashimoto, K.** 1971. Langerhans' cell granule. An endocytotic organelle. Arch. Dermatol. **104:**148–160.
29. **Hogquist, K. A., S. C. Jameson, W. R. Heath, J. L. Howard, M. J. Bevan, and F. R. Carbone.** 1994. T cell receptor antagonist peptides induce positive selection. Cell **76:**17–27.
30. **Hunger, R. E., P. A. Sieling, M. T. Ochoa, M. Sugaya, A. E. Burdick, T. H. Rea, P. J. Brennan, J. T. Belisle, A. Blauvelt, S. A. Porcelli, and R. L. Modlin.** 2004. Langerhans cells utilize CD1a and langerin to efficiently present nonpeptide antigens to T cells. J. Clin. Investig. **113:**701–708.
31. **Juhlin, L., and W. B. Shelley.** 1977. New staining techniques for the Langerhans cell. Acta Derm. Venereol. **57:**289–296.
32. **Kanbe, T., Y. Han, B. Redgrave, M. H. Riesselman, and J. E. Cutler.** 1993. Evidence that mannans of *Candida albicans* are responsible for adherence of yeast forms to spleen and lymph node tissue. Infect. Immun. **61:**2578–2584.
33. **Kitano, Y., and N. Okada.** 1983. Separation of the epidermal sheet by dispase. Br. J. Dermatol. **108:**555–560.
34. **Koch F., E. Kämpgen, G. Schuler, and N. Romani.** 2001. Isolation, enrichment and culture of murine epidermal Langerhans cells, p. 43-62. *In* S. P. Robinson and A. J. Stagg (ed.), Dendritic cell protocols. Humana Press, Totowa, N.J.
35. **Kress, C., S. Vandormael-Pournin, P. Baldacci, M. Cohen-Tannoudji, and C. Babinet.** 1998. Nonpermissiveness for mouse embryonic stem (ES) cell derivation circumvented by a single backcross to 129/Sv strain: establishment of ES cell lines bearing the Omd conditional lethal mutation. Mamm. Genome **9:**998-1001.
36. **Kyburz, D., P. Aichele, D. E. Speiser, H. Hengartner, R. M. Zinkernagel, and H. Pircher.** 1993. T cell immunity after a viral infection versus T cell tolerance induced by soluble viral peptides. Eur. J. Immunol. **23:**1956–1962.
37. **Labuda, M., J. M. Austyn, E. Zuffova, O. Kozuch, N. Fuchsberger, J. Lysy, and P. A. Nuttall.** 1996. Importance of localized skin infection in tick-borne encephalitis virus transmission. Virology **219:**357-366.
38. **Mc Dermott, R., U. Ziylan, D. Spehner, H. Bausinger, D. Lipsker, M. Mommaas, J. P. Cazenave, G. Raposo, B. Goud, H. de la Salle, J. Salamero, and D. Hanau.** 2002. Birbeck granules are subdomains of endosomal recycling compartment in human epidermal Langerhans cells, which form where Langerin accumulates. Mol. Biol. Cell **13:**317-335.
39. **McLellan, A. D., M. Kapp, A. Eggert, C. Linden, U. Bommhardt, E. B. Brocker, U. Kammerer, and E. Kampgen.** 2002. Anatomic location and T-cell stimulatory functions of mouse dendritic cell subsets defined by CD4 and CD8 expression. Blood **99:**2084-2093.
40. **Mellman, I., and R. M. Steinman.** 2001. Dendritic cells: specialized and regulated antigen processing machines. Cell **106:**255-258.
41. **Mizumoto, N., and A. Takashima.** 2004. CD1a and langerin: acting as more than Langerhans cell markers. J. Clin. Investig. **113:**658-660.
42. **Moll, H., S. Flohe, and M. Rollinghoff.** 1995. Dendritic cells in Leishmania major-immune mice harbor persistent parasites and mediate an antigen-specific T cell immune response. Eur. J. Immunol. **25:**693-699.
43. **Moll, H., H. Fuchs, C. Blank, and M. Rollinghoff.** 1993. Langerhans cells transport Leishmania major from the infected skin to the draining lymph node for presentation to antigen-specific T cells. Eur. J. Immunol. **23:**1595-1601.
44. **Mommaas, M., A. Mulder, B. J. Vermeer, and F. Koning.** 1994. Functional human epidermal Langerhans cells that lack Birbeck granules. J. Investig. Dermatol. **103:**807-810.
45. **Moody, D. B., and S. A. Porcelli.** 2003. Intracellular pathways of CD1 antigen presentation. Nat. Rev. Immunol. **3:**11-22.
46. **Moore, M. W., F. R. Carbone, and M. J. Bevan.** 1988. Introduction of soluble protein into the class I pathway of antigen processing and presentation. Cell **54:**777-785.
47. **Nigou, J., C. Zelle-Rieser, M. Gilleron, M. Thurnher, and G. Puzo.** 2001. Mannosylated lipoarabinomannans inhibit IL-12 production by human dendritic cells: evidence for a negative signal delivered through the mannose receptor. J. Immunol. **166:**7477-7485.
48. **Oxenius, A., M. F. Bachmann, R. M. Zinkernagel, and H. Hengartner.** 1998. Virus-specific MHC-class II-restricted TCR-transgenic mice: effects on humoral and cellular immune responses after viral infection. Eur. J. Immunol. **28:**390-400.
49. **Pooley, J. L., W. R. Heath, and K. Shortman.** 2001. Cutting edge: intravenous soluble antigen is presented to CD4 T cells by CD8− dendritic cells, but cross-presented to CD8 T cells by CD8+ dendritic cells. J. Immunol. **166:**5327-5330.
50. **Quintanilla, M., K. Brown, M. Ramsden, and A. Balmain.** 1986. Carcinogen-

specific mutation and amplification of Ha-ras during mouse skin carcinogenesis. Nature **322:**78-80.
51. **Riedl, E., Y. Tada, and M. C. Udey.** 2004. Identification and characterization of an alternatively spliced isoform of mouse Langerin/CD207. J. Investig. Dermatol. **123:**78-86.
52. **Ritter, U., A. Meissner, C. Scheidig, and H. Korner.** 2004. CD8alpha- and Langerin-negative dendritic cells, but not Langerhans cells, act as principal antigen-presenting cells in leishmaniasis. Eur. J. Immunol. **34:**1542-1550.
53. **Romani, N., S. Holzmann, C. H. Tripp, F. Koch, and P. Stoitzner.** 2003. Langerhans cells-dendritic cells of the epidermis. APMIS **111:**725-740.
54. **Romani, N., G. Stingl, E. Tschachler, M. D. Witmer, R. M. Steinman, E. M. Shevach, and G. Schuler.** 1985. The Thy-1-bearing cell of murine epidermis. A distinctive leukocyte perhaps related to natural killer cells. J. Exp. Med. **161:**1368-1383.
55. **Sacks, D., and N. Noben-Trauth.** 2002. The immunology of susceptibility and resistance to Leishmania major in mice. Nat. Rev. Immunol. **2:**845-858.
56. **Sahly, H., and R. Podschun.** 1997. Clinical, bacteriological, and serological aspects of *Klebsiella* infections and their spondylarthropathic sequelae. Clin. Diagn. Lab. Immunol. **4:**393-399.
57. **Salamero, J., H. Bausinger, A. M. Mommaas, D. Lipsker, F. Proamer, J. P. Cazenave, B. Goud, H. de la Salle, and D. Hanau.** 2001. CD1a molecules traffic through the early recycling endosomal pathway in human Langerhans cells. J. Investig. Dermatol. **116:**401-408.
58. **Schwenk, F., U. Baron, and K. Rajewsky.** 1995. A cre-transgenic mouse strain for the ubiquitous deletion of loxP-flanked gene segments including deletion in germ cells. Nucleic Acids Res. **23:**5080-5081.
59. **Scott, P., and C. A. Hunter.** 2002. Dendritic cells and immunity to leishmaniasis and toxoplasmosis. Curr. Opin. Immunol. **14:**466-470.
60. **Spath, G. F., and S. M. Beverley.** 2001. A lipophosphoglycan-independent method for isolation of infective Leishmania metacyclic promastigotes by density gradient centrifugation. Exp. Parasitol. **99:**97-103.
61. **Stambach, N. S., and M. E. Taylor.** 2003. Characterization of carbohydrate recognition by langerin, a C-type lectin of Langerhans cells. Glycobiology **13:**401-410.
62. **Stoitzner, P., S. Holzmann, A. D. McLellan, L. Ivarsson, H. Stossel, M. Kapp, U. Kammerer, P. Douillard, E. Kampgen, F. Koch, S. Saeland, and N. Romani.** 2003. Visualization and characterization of migratory Langerhans cells in murine skin and lymph nodes by antibodies against Langerin/CD207. J. Investig. Dermatol. **120:**266-274.
63. **Stössel, H., F. Koch, E. Kampgen, P. Stoger, A. Lenz, C. Heufler, N. Romani, and G. Schuler.** 1990. Disappearance of certain acidic organelles (endosomes and Langerhans cell granules) accompanies loss of antigen processing capacity upon culture of epidermal Langerhans cells. J. Exp. Med. **172:**1471-1482.
64. **Sugita, M., N. van Der Wel, R. A. Rogers, P. J. Peters, and M. B. Brenner.** 2000. CD1c molecules broadly survey the endocytic system. Proc. Natl. Acad. Sci. USA **97:**8445-8450.
65. **Tailleux, L., O. Schwartz, J. L. Herrmann, E. Pivert, M. Jackson, A. Amara, L. Legres, D. Dreher, L. P. Nicod, J. C. Gluckman, P. H. Lagrange, B. Gicquel, and O. Neyrolles.** 2003. DC-SIGN is the major Mycobacterium tuberculosis receptor on human dendritic cells. J. Exp. Med. **197:**121-127.
66. **Takahashi, S., and K. Hashimoto.** 1985. Derivation of Langerhans cell granules from cytomembrane. J. Investig. Dermatol. **84:**469-471.
67. **Tripp, C. H., S. Chang-Rodriguez, P. Stoitzner, S. Holzmann, H. Stossel, P. Douillard, S. Saeland, F. Koch, A. Elbe-Burger, and N. Romani.** 2004. Ontogeny of Langerin/CD207 expression in the epidermis of mice. J. Investig. Dermatol. **122:**670-672.
68. **Turville, S. G., P. U. Cameron, A. Handley, G. Lin, S. Pohlmann, R. W. Doms, and A. L. Cunningham.** 2002. Diversity of receptors binding HIV on dendritic cell subsets. Nat. Immunol. **3:**975-983.
69. **Udey, M. C., E. von Stebut, S. Mendez, D. L. Sacks, and Y. Belkaid.** 2001. Skin dendritic cells in murine cutaneous leishmaniasis. Immunobiology **204:** 590-594.
70. **Valladeau, J., V. Clair-Moninot, C. Dezutter-Dambuyant, J. J. Pin, A. Kissenpfennig, M. G. Mattei, S. Ait-Yahia, E. E. Bates, B. Malissen, F. Koch, F. Fossiez, N. Romani, S. Lebecque, and S. Saeland.** 2002. Identification of mouse langerin/CD207 in Langerhans cells and some dendritic cells of lymphoid tissues. J. Immunol. **168:**782-792.
71. **Valladeau, J., C. Dezutter-Dambuyant, and S. Saeland.** 2003. Langerin/CD207 sheds light on formation of birbeck granules and their possible function in Langerhans cells. Immunol. Res. **28:**93-107.
72. **Valladeau, J., O. Ravel, C. Dezutter-Dambuyant, K. Moore, M. Kleijmeer, Y. Liu, V. Duvert-Frances, C. Vincent, D. Schmitt, J. Davoust, C. Caux, S. Lebecque, and S. Saeland.** 2000. Langerin, a novel C-type lectin specific to Langerhans cells, is an endocytic receptor that induces the formation of Birbeck granules. Immunity **12:**71-81.
73. **Vremec, D., J. Pooley, H. Hochrein, L. Wu, and K. Shortman.** 2000. CD4 and CD8 expression by dendritic cell subtypes in mouse thymus and spleen. J. Immunol. **164:**2978-2986.
74. **Weinlich, G., M. Heine, H. Stossel, M. Zanella, P. Stoitzner, U. Ortner, J. Smolle, F. Koch, N. T. Sepp, G. Schuler, and N. Romani.** 1998. Entry into afferent lymphatics and maturation in situ of migrating murine cutaneous dendritic cells. J. Investig. Dermatol. **110:**441-448.
75. **Wolff, K.** 1967. The fine structure of the Langerhans cell granule. J. Cell Biol. **35:**468-473.
76. **Wu, S. J., G. Grouard-Vogel, W. Sun, J. R. Mascola, E. Brachtel, R. Putvatana, M. K. Louder, L. Filgueira, M. A. Marovich, H. K. Wong, A. Blauvelt, G. S. Murphy, M. L. Robb, B. L. Innes, D. L. Birx, C. G. Hayes, and S. S. Frankel.** 2000. Human skin Langerhans cells are targets of dengue virus infection. Nat. Med. **6:**816-820.
77. **Zhang, Y., A. Harada, J. B. Wang, Y. Y. Zhang, S. Hashimoto, M. Naito, and K. Matsushima.** 1998. Bifurcated dendritic cell differentiation in vitro from murine lineage phenotype-negative c-kit+ bone marrow hematopoietic progenitor cells. Blood **92:**118-128.
78. **Zhang, Y., Y. Y. Zhang, M. Ogata, P. Chen, A. Harada, S. Hashimoto, and K. Matsushima.** 1999. Transforming growth factor-beta1 polarizes murine hematopoietic progenitor cells to generate Langerhans cell-like dendritic cells through a monocyte/macrophage differentiation pathway. Blood **93:** 1208-1220.